NOAA Technical Memorandum NOS NGS- 55

KINEMATIC GPS RESULTS WITHOUT STATIC INITIALIZATION

Benjamin W. Remondi

Rockville, MD

May 1991

U.S. DEPARTMENT OF COMMERCE / National Oceanic and Atmospheric Administration / National Ocean Service / Coast and Geodetic Survey

NOAA TECHNICAL PUBLICATIONS

National Ocean Service/National Geodetic Survey Subseries

The National Geodetic Survey (NGS), Coast and Geodetic Survey, the National Ocean Service (NOS), NOAA, establishes and maintains the basic national horizontal, vertical, and gravity networks of geodetic control, and provides Government-wide leadership in the improvement of geodetic surveying methods and instrumentation; coordinates operations to assure network development; and provides specifications and criteria for survey operations by Federal, State, and other agencies.

NGS engages in research and development for the improvement of knowledge of the figure of the Earth and its gravity field, and has the responsibility to procure geodetic data from all sources, process these data, and make them generally available to users through a central data base.

Geodetic publications of NOAA and the Coast and Geodetic Survey are sold in paper form by the National Geodetic Information Center. To obtain a price list or to place an order contact:

National Geodetic Information Center (N/CG174)
Coast and Geodetic Survey
National Ocean Service
National Oceanic and Atmospheric Administration
Rockville, MD 20852

Telephone: 1 301 443 8631

When placing an order, make check or money order payable to: National Geodetic Survey. Do not send cash or stamps. Publications can be charged to Visa or MasterCard, or purchased over the counter at the National Geodetic Information Center, 11400 Rockville Pike, Room 24, Rockville, MD.

An excellent reference source for all Government publications is the National Depository Library Program, a network of about 1,400 designated libraries. Requests for borrowing Depository Library material may be made through your local library. A free listing of libraries in this system is available from the Library Division, U.S. Government Printing Office, Washington, DC 20401 (telephone: 1 202 275 3635).

NOAA Technical Memorandum NOS NGS - 55

KINEMATIC GPS RESULTS
WITHOUT
STATIC INITIALIZATION

Benjamin W. Remondi

Rockville, MD

May 1991

For Sale by the National Geodetic Information Center, NOAA
Rockville, MD 20852

UNITED STATES
DEPARTMENT OF COMMERCE
Robert A. Mosbacher,
Secretary

National Oceanic and
Atmospheric Administration
John A. Knauss,
Under Secretary

National Ocean Service
Virginia K. Tippie,
Asst. Administrator

Coast and Geodetic Survey
R. Adm. J. Austin Yeager,
Director

CONTENTS

KINEMATIC GPS RESULTS WITHOUT STATIC INITIALIZATION

Benjamin W. Remondi
National Geodetic Survey
National Ocean Service, NOAA
Coast and Geodetic Survey
Rockville, MD 20852

ABSTRACT. The kinematic Global Positioning System (GPS) technique, developed between 1983-1985, has delivered centimeter-level trajectory determination as promised. This has been satisfactory for survey operations because the static initialization process, to establish carrier phase integer ambiguities, is acceptable. The author discusses an approach developed in early 1990 which allows the initialization step to be accomplished while in motion. This paper focusses on results achieved from late 1990 to the present.

Numerous kinematic experiments have been performed. Using the kinematic receiver, the operator periodically visits a known survey monument so that, during postprocessing, kinematic truth will be known. Typically, a reference receiver is situated close (less than 1 km) to the rover receiver, and other reference receivers are situated at remote sites (e.g., 13 km). The data are then processed using "kinematic GPS without static initialization". The resulting trajectory is compared against the truth trajectory to verify that correct integer lanes have been isolated and to determine the accuracies achieved at the various experimental distances.

INTRODUCTION

Kinematic GPS based on the carrier phase was developed in 1983-85 (Remondi 1985a, 1985b). This was undertaken primarily to develop methods for centimeter-level trajectory determination and, as a byproduct, "stop-and-go" kinematic survey. Real-time aspects were discussed. The primary obstacles to real time centimeter navigation were cycle slips, the static initialization requirement, and the need to transmit observations from the reference to the rover.

Over the past 3 to 5 years GPS investigators have realized that static initialization is not required. Many articles address this possibility (Seeber and Wubbena 1989, Loomis 1989, Hatch 1990, Hein et al. 1990, Hwang 1990, Remondi 1990, Mader 1990, Rocken et al. 1990, DeLoach 1991). In particular the paper by Hatch (1990) is interesting in that it presents a new procedure and discusses other contemporary papers on the subject.

With regard to cycle slips, it is clear that GPS receivers, especially dedicated-channel GPS receivers, have advanced tremendously. Not only are the cycle slips becoming fewer but also flags, internal to the receiver, provide confidence levels with respect to cycle slips. One can

anticipate a day when there will be very few cycle slips and so many GPS, Glonass, Inmarsat, and other satellites that cycle slips will be irrelevant, in that only the fractional phase will be required (at least over tens of kilometers).

This paper presents an approach to kinematic GPS without static initialization. Brief reference to this method was made in a May 1990 National Geodetic Survey Technical Memorandum (Remondi, 1990). The analysis was performed between December 1989 and February 1990. Although this method is unlike others presented to date, it seems similar to that of Mr. Ron Hatch (1990) in its exploitation of the geometry and physics.

Although my approach to kinematic GPS without static initialization (hereafter referred to as "on-the-fly" or OTF) will be given here, it is my intention to highlight the results rather than the method. Algorithms need to be fast, simple, and discriminating, but in this discussion results are primary and efficiency secondary. At the present time the computations have not been optimized; this is temporary as it is obvious how to make the algorithm efficient. In evaluating the method no adverse decision should be made based on computational time as processing will, ultimately, be accomplished in seconds. The factors of highest interest are: the minimum number of satellites, the shortest time span required as a function of the number of satellites, the greatest distance the remote kinematic receiver can be from the reference receiver as a function of the number of satellites and the observation time span, the dynamical extremes, and the extremes with regard to the tropospheric and ionospheric delays. This paper provides initial results for distances up to 13 km using five to six satellites. Remarks regarding seven, eight, or more satellites will be made. Other considerations of interest are cited as well.

Results from smoothing the code with the carrier are included. This is in itself interesting as it indicates what accuracy levels can be expected for (code/carrier) differential navigation over longer distances. Based on the results herein, 1 m (rms) C/A differential code/carrier navigation seems readily achievable. Based on limited processing of P code and carrier, 0.25 m (rms) also seems achievable. Naturally these results depend on the number of satellites tracked, the time span of the carrier and code mapping, and other factors. For long time spans the effects of multipath can be largely averaged away, whereas for short time spans multipath can be the predominate error source.

THEORY

Code and Carrier

It is well known (Hatch 1982) that both carrier and code provide ranges or pseudoranges. The main difference is that carrier pseudoranges have an initial bias which needs to be established in order to bring carrier phase measurements up to full usefulness. In fact (intentionally omitting subscripts and superscripts)

$$-\phi = \rho/\lambda + n + e_{\phi} \tag{1}$$

$$R = \rho + e_R \tag{2}$$

are the fundamental or conceptual double difference equations where ϕ is the carrier phase

measurement, R is the code pseudorange, ρ is the modeled range, λ is the carrier wavelength, n is the initial carrier phase "integer" bias, and e is measurement noise. If we have code and carrier at t_1 and t_2 we can create their difference in time:

$$\phi(t_1) - \phi(t_2) = [\rho(t_2) - \rho(t_1)]/\lambda + e_\phi(t_2) - e_\phi(t_1) \tag{3}$$

$$R(t_2) - R(t_1) = \rho(t_2) - \rho(t_1) + e_R(t_2) - e_R(t_1) \tag{4}$$

equating the ρ's we get:

$$[\phi(t_1) - \phi(t_2)]\lambda + e^*_\phi = [R(t_2) - R(t_1)] + e^*_R \tag{5}$$

and finally

$$R(t_1) = R(t_2) - [\phi(t_1) - \phi(t_2)]\lambda + e \tag{6}$$

In words, the highly accurate carrier phase at t_1 and t_2 can be used to map $R(t_2)$ to time t_1. This provides a method of sampling $R(t_1)$ many times over. The method assumes no cycle slips on a satellite to be mapped forward or backwards in time to t_1. In these simplified equations the e's represent measurement error and unmodeled effects. Carrier pseudorange measurement noise is on the order of 1 cm, whereas C/A code pseudorange measurement noise is on the order of 2 m.

Kinematic GPS With Static Initialization

Kinematic GPS with static initialization has been fully documented in the literature (Remondi 1985a, 1985b, 1988). For receivers 1 and 2 occupying known marks a and b we have the double difference carrier equation:

$$t_{ref}: \quad -\phi_{12}^{jk} = \rho_{ab}^{jk} + n_{12}^{jk} \tag{7}$$

At a later time (or earlier) t_i assume that receiver 1 remains at mark a and that receiver 2 has moved to point c_i in three-dimensional space, not necessarily at a monument. Thus:

$$t_i: \quad -\phi_{12}^{jk} = \rho_{ac}^{jk} + n_{12}^{jk} \tag{8}$$

In these last two equations the ρ's are intentionally in units of cycles and the double difference indices are explicitly displayed. On the assumption of no cycle slips, the n_{12}^{jk} stay constant during all kinematic activities. If four or more satellites are tracked between t_{ref} and t_i the n_{12}^{jk} can be computed from eq. (7) and used in eq. (8) to compute the position of point c_i. In practice, the actual solution of the integers gives real values close to integers. Rounding is subsequently performed to obtain exact integer values. On subtracting eqs. (7) and (8) we get:

$$\rho_c^{jk}(t_i) = \rho_a^{jk}(t_i) + \rho_{ab}^{jk}(t_{ref}) + \phi_{12}^{jk}(t_{ref}) - \phi_{12}^{jk}(t_i) \tag{9}$$

Thus, clearly, c_i can be computed without specific knowledge of the integers. This latter solution will not be as accurate as the former. One might use this approach when position b is not sufficiently well known to fix the ambiguities to integers. In fact this latter equation will be used to project candidate solutions forward and backwards. Once position c_i is computed, eq. (8) is used to compute real-valued ambiguities which are subsequently checked for closeness to integers.

Kinematic GPS Without Static Initialization

Kinematic GPS without static initialization is only slightly more complex than kinematic GPS with static initialization presented above. In this case we rely on the carrier-smoothed code to provide an initial guess to within a few meters (e.g., 2 m for C/A code and 0.5 m for P code). Trial and elimination is used to evaluate candidate positions within a specified volumetric neighborhood of this initial solution. Conceptually, every cubic centimeter within a 4m•4m•4m volume could be examined. Here is how a trial will be evaluated. Use eq. (9) to project the assumed known point b (i.e., the candidate position at t_{ref}) forward or backward in time to each observation epoch t_i over the time period selected or available. This will yield a position c_i at each epoch t_i. Then substitute position c_i into eq. (8), above, to compute the n_{12}^{jk} . Success will be decided if the ambiguities are approximately integer values at all the selected epochs. This is the conceptual method suggested in the referenced NGS Technical Memorandum (Remondi 1990). What ultimately discriminates candidate solutions is the integrated carrier Doppler shift. Given a sufficiently long time span, only the correct starting position (or, equivalently, the correct lanes) will yield an integrated Doppler history which agrees with the carrier observations.

In practice every cubic centimeter is not evaluated to avoid unnecessary computations. Instead the candidates are selected as the points of intersection of three double difference planes. This is a natural procedure that could also have been used in pseudo-kinematic (p-k) processing (Remondi 1990). I expressly decided not to use this procedure (for p-k) to define my candidates for a several reasons: (1) for p-k processing it is not needed since huge search volumes can be processed in a matter of seconds where grid of points separated by $\lambda/4$ in each dimension is evaluated on the first pass and (2) there is a risk in defining candidates this way. The risk is that if the phase measurements at the defining epoch are in error then the candidates will also be. True, there are ways to overcome this. For example, use kinematic triple differences on N neighboring epochs to validate that observations (at the defining epoch) have small measurement errors. Should the kinematic triple difference residuals be large another defining reference epoch would be selected and the procedure repeated. In short, forming trials by the intersection of double-difference planes is not essential in p-k processing but is extremely helpful in OTF processing. The kinematic triple-difference validation procedure described above could also be applied to validating the OTF candidates at the defining epoch.

The intersection of double-difference planes can be accomplished with a variety of observables. With L1 this process yields a three-dimensional lattice of candidates based on the intersection of 19 cm lanes. Assuming the planes to be perpendicular yields 68,921 candidates in a cube based on ±3.8 m from the initial guess. This is certainly preferred to evaluating every cubic centimeter since there are 440,711,081 such candidates. Even a 5-centimeter lattice defines 3,581,577 candidates. It should be stated that, based on results given in this paper, a ±3.8-meter

box may not be necessary on the first attempt and ±1.9 m might be adequate. That would reduce the number of candidates by a factor of 8.

Dual frequency P code receivers provide two immediately obvious advantages: (1) the carrier-smoothed code determined solution can be safely assumed to be within, say, 1.72 m, at least for the first pass (even half of that would be reasonable); and (2) one can form the L1-L2 observable with an 86 centimeter wide-lane wavelength. Thus, at most, 125 candidates would need to be evaluated.

In this investigation I concentrate on dual frequency C/A code receivers where the observed L1 wavelength is 19 cm and the observed L2 wavelength is 12.2 cm. The candidates at the defining epoch are generated using L1 (19 cm), L34: L1-L2 (34 cm), L43: 2•L1-L2 (43 cm), and L163: L34-L43 (163 cm). With a ±3.8-meter box, the intersection of 34-centimeter lanes could yield up to 12,167 candidates. In such a box the intersection of 163-centimeter lanes would yield up to 125 candidates. In practice, however, observables formed as differences of raw observations and differences of differences are noisy, complicating this simple presentation. In spite of this, most of the results given here are based on using the 163-centimeter double-wide lane. The remainder of the results are based on using the 19-centimeter narrow lane. Success has been achieved using the 34-centimeter lane, but that will not be discussed here.

How does one isolate the correct lanes? Start with a candidate position b (at t_{ref}), derived from the intersection of three double-difference planes, and compute the position c (at t_i), using eq. (9) . Substitute c into eq. (8) to get real-valued ambiguities. Associated with each candidate b is a sum over all double differences and over all selected epochs within the selected time span. For a given double difference, at a given epoch, the value to be accumulated is:

$$0.5 - |n_{integer} - n_{real\text{-}value}|$$

Clearly if $n_{real\text{-}value}$ happened to be an integer an increment of 0.5, exactly, would be accumulated. This is equivalent to using the ambiguity function method. The objective is to isolate the candidate for which this sum is the largest. That will be referred to as "peak1" in the section on results.

EXPERIMENTS TO TEST OTF

I have concentrated on dual frequency C/A code receivers because the National Geodetic Survey (NGS) and the U.S. Army Corps of Engineers (USACOE) intend to use them for initial operations based upon this technology. Although this technique works better with P code receivers, scant mention will be made of them. The algorithms and software programs that are used for C/A code receivers apply to P code receivers as well.

The first experimental data of relevance to this investigation were, in fact, dual frequency P code data from the Jet Propulsion Laboratory (JPL) Rogue receivers. This is a 10-minute data set comprising eight satellites collected at Scripps Institute of Oceanography during December 1989 (Rocken 1990). These data were provided to NGS by Dr. Thomas M. Kelecy of the University of Colorado, Boulder, CO. It was processed as a first test of the recently developed

OTF processing software. This processing was accomplished in the fall of 1990. Since this investigation does not concern P code data I shall limit my remarks.

The pseudoranges from this 10-minute sample of data were remarkable. The P code ranges carrier-mapped to the selected reference epoch yielded individual positions, at the reference epoch, typically less than 50 cm. The average of these mapped values was accurate at the 1 to 2-decimeter level. Thus, in this case, wide lane (86 cm) integers could be fixed without a lane search. Once they were fixed to integers the position at the reference epoch could be recomputed and the narrow lanes generated. Finally the entire 10-minute trajectory was computed accurately to the centimeter level. These results were also achieved by first using seven and then using six out of eight satellites. In summary, if this single 10-minute sample is a representative one, then the value of P code receivers for OTF technology is apparent.

Many dual frequency C/A code experiments were performed between July 1990 and March 1991 with Ashtech and Trimble GPS receivers.

Experiment A

Of the four data sets taken with NGS Trimble receivers in July 1990, the July 16 experiment was selected for evaluation as it was the most complex and, therefore, most interesting. The others are currently being processed but will not be reported here. There appears to be no differences in the results achieved so far for these other experiments. During the experiments in July 1990, the selective availability (S/A) feature was on.

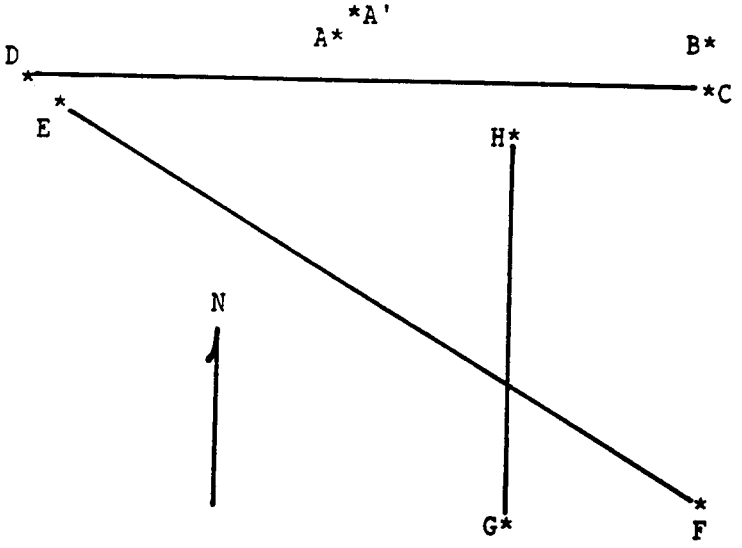

Figure 1.--Kinematic survey course for experiment A.

I shall refer to the July 16, 1990 two-receiver experiment as experiment A. This data set was, in fact, a NGS kinematic survey data set performed with OTF processing in mind. An airport in Michigan served as the course. Figure 1 depicts this three-runway airport along with the relevant survey marks. The reference receiver occupied site A except for two beginning and two

ending antenna swaps between mark A and temporary mark A'. Table 1 lists the kinematic survey occupation log for the ROVER.

Table 1.--Survey site-occupation log based on 15-second epochs, July 16, 1990

Mark	Epochs at Mark	Mark	Epochs at Mark
A'	0 - 8	C	170 - 177
A	13 - 18	D	188 - 196
A'	21 - 26	E	202 - 210
B	39 - 48	F	221 - 228
C	54 - 63	G	237 - 246
D	71 - 79	H	259 - 267
E	84 - 92	B	273 - 281
F	103 - 110	A'	290 - 296
G	120 - 129	A	298 - 302
H	141 - 150	A'	306 - 311
B	156 - 165		

During experiment A either five or six satellites were tracked at all times as shown, simply, in Table 2. Observations were taken on 15-second epochs; the data collection period is 77.5 min.

Table 2.--Satellite visibility table for experiment A, July 16, 1990

Epochs	Satellites Tracked	No. satellites
0-166	02 06 09 11 13	5
167-232	02 06 09 11 12 13	6
233-238	06 09 11 12 13	5
239-311	06 09 11 12 13 14	6

Figure 2 shows the PDOP curve for experiment A. PDOP was not an important factor in experiment A but it was a factor in experiment B.

Finally, figure 3 illustrates the horizontal trajectory computed from the collected observations based on kinematic GPS postprocessing. The results of OTF processing are discussed in the section entitled results.

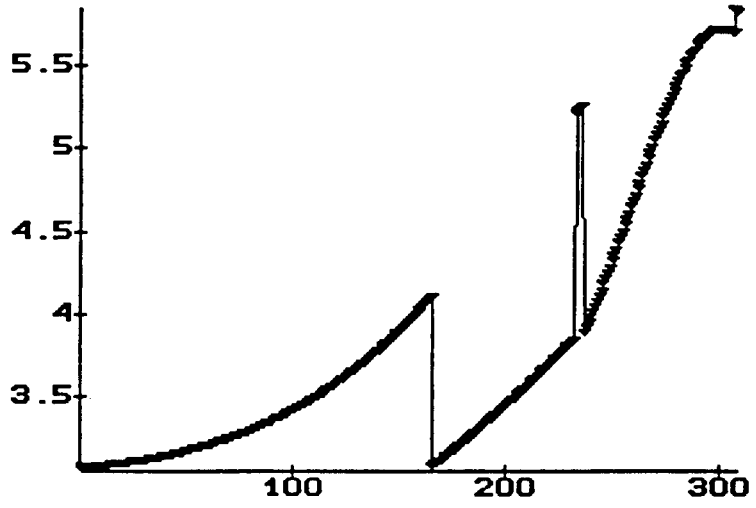

Figure 2.--Plot of PDOP versus 15-second epochs
for experiment A, July 16, 1990.

Experiment B

During this past winter numerous kinematic experiments were performed with Ashtech and Trimble dual frequency C/A code receivers as a part of this OTF investigation. All of these experiments eventually will be processed either by the author or personnel at USACOE and documented. The first of these winter experiments to be processed in great detail was performed on February 17, 1991 at the National Institute of Standards and Technology (NIST). Four NGS Trimble SST receivers were used. This is the same kind of receiver used for experiment A described above.

The experimental course, depicted in figure 4, placed receivers at survey marks NBS3, SCHL, and CLRK. These receivers were stationary throughout the experiment. Monument NBS3 and the depicted kinematic survey course (i.e., marks A-G and NBS5) are located at the NIST, a fitting place for such experiments. The kinematic course, located roughly 0.5 km west of NBS3, is traversed by a fourth receiver, the ROVER receiver.

The ROVER followed this kinematic course for approximately 5 hours. Whether occupying a survey mark or in motion, the receiver tracked all available satellites at all times. The kinematic portion of figure 4, which is not to scale, would fit within a 200-meter circle. The distances from NIST to SCHL and NIST to CLRK are 8 km and 13 km, respectively. The ROVER occupied a kinematic mark from five to eight times during the experiment. The only a priori information available for the postprocessing were the precise positions of NBS3 and NBS5. Observations were collected on 2-second epochs.

During this experiment five to seven satellites were tracked at all times. I have chosen to ignore PRN 9 in the processing, primarily to show the results achievable with only five or six satellites. (The data are currently being reprocessed using PRN 9, but those results will not be

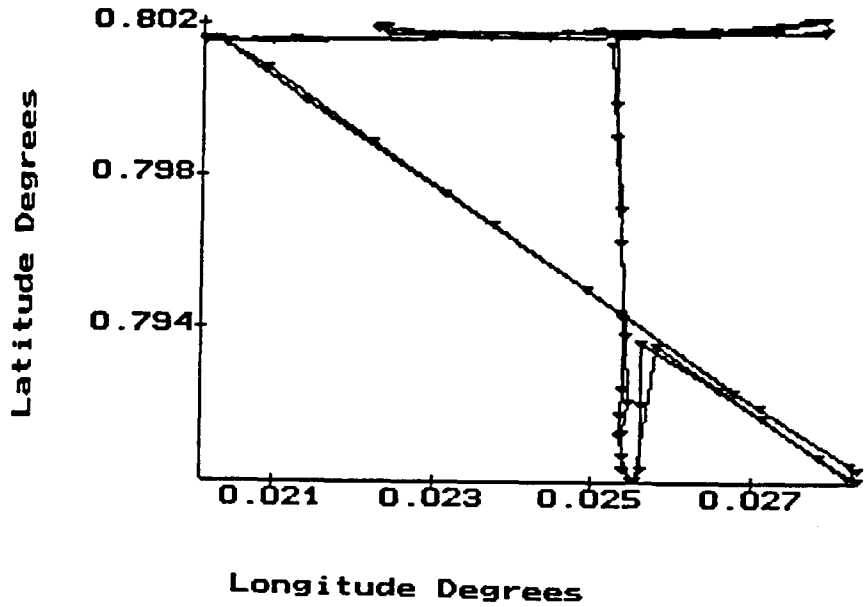

Figure 3.--Horizontal plot of kinematic trajectory for experiment A, July 16, 1990.

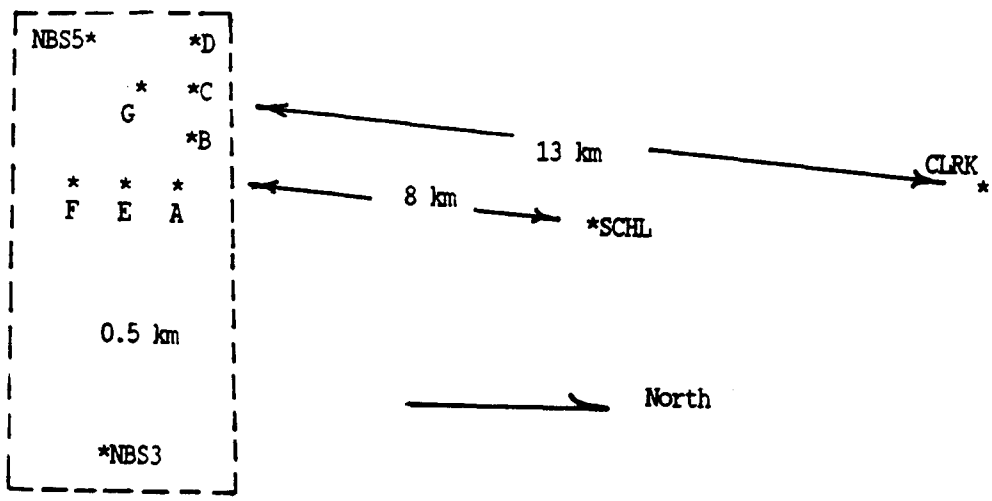

Figure 4.--Kinematic survey course for experiment B, February 17, 1991.

included; clearly data from seven satellites improve matters considerably.) Table 3 lists the satellite visibility during experiment B. The column on the far right includes the number of satellites visible at a given epoch. This table is based on 20-second epochs even though the measurements were taken every 2 seconds.

Table 3.--Satellite visibility for experiment B,
February 17, 1991

Epochs	Satellites tracked	No. satellites
0 - 47	02 11 15 18 19	5
48 - 87	02 06 11 15 18 19	6
88 - 327	02 06 11 15 19	5
328 - 383	02 06 11 13 15 19	6
384 - 471	02 06 13 15 19	5
472 - 479	02 06 13 14 15 19	6
480 - 655	02 06 13 14 15	5
656 - 799	02 06 12 13 14 15	6
800 - 888	02 06 12 13 14 15	5

Figure 5 displays the PDOP curve for the 5-hour duration of experiment B. It is based on 20-second epochs so as to agree with table 3.

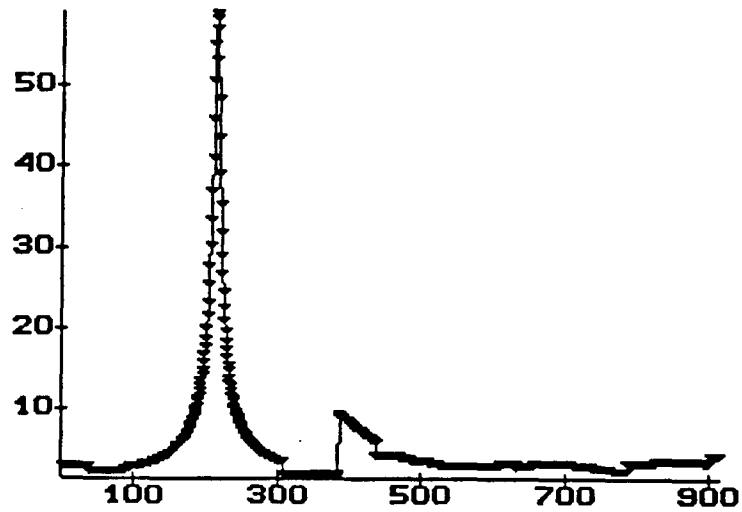

Figure 5.--Plot of PDOP versus 20-second epochs
for experiment B, February 17, 1991.

Table 4 shows the survey occupation log for experiment B.

Finally, figure 6 displays the horizontal trajectory of the ROVER for the entire 5-hour trajectory. This trajectory was computed by standard kinematic GPS processing of NBS3 and ROVER carrier phase data. This same trajectory was generated using OTF postprocessing with no a priori information and without benefitting from the fact that the ROVER stopped to occupy survey marks. Actually there was no need to stop. No cycle slips occurred during this

Table 4.--Survey site-occupation log for experiment B
based on 20-second epochs, February 17, 1991

Mark	Epochs occupied	Mark	Epochs occupied
KINA	000 - 011	KIND	460 - 468
KINE	021 - 029	KINC	475 - 484
KINF	041 - 050	KINB	491 - 500
KIND	061 - 071	KINA	507 - 516
KINC	080 - 089	NBS5	525 - 534
KINB	099 - 109	KING	542 - 551
KINA	119 - 130	KINE	559 - 568
NBS5	142 - 152	KINF	574 - 583
KING	161 - 171	KIND	594 - 603
KINE	182 - 192	KINC	609 - 618
KINF	199 - 208	KINB	625 - 634
KIND	219 - 229	KINA	639 - 648
KINC	235 - 245	NBS5	657 - 667
KINB	253 - 262	KING	676 - 685
KINA	268 - 279	KINE	696 - 705
NBS5	288 - 298	KINF	717 - 726
KING	306 - 315	KIND	740 - 749
KINE	323 - 332	KINC	757 - 766
KINF	338 - 347	KINB	773 - 782
KIND	357 - 366	KINA	787 - 797
KINC	374 - 382	NBS5	808 - 819
KINB	392 - 401	KING	827 - 836
KINA	409 - 417	KINE	846 - 855
KINE	424 - 433	KINF	862 - 871
KINF	440 - 445	KINA	882 - 888

experiment except for just-rising or just-setting satellites. OTF processing of these data was performed down to elevations of 10°. I consider this to be difficult over 13 km when codeless/squared L2 observations are used, because they are very noisy. In spite of this, OTF processing was still successful, as will be shown later.

Discussion

Although the selection of these two experiments was arbitrary, there is no indication that the results achieved would be different using other experiments. Experiment A was performed 6 months earlier than experiment B; experiment A was executed at noon, whereas experiment B commenced at midnight; experiment A was carried out during S/A, but experiment B was not. These two were selected simply because they were the first C/A code dual frequency (with squared L2) kinematic experiments to be processed using new OTF postprocessing software.

METHODOLOGY

This section describes how the experimental data, discussed above, is used to demonstrate OTF kinematic GPS postprocessing. All data were collected using kinematic GPS. Thus the satellites were tracked whether the rover was moving or stationary. Traditionally such kinematic GPS data are processed based on a static initialization step.

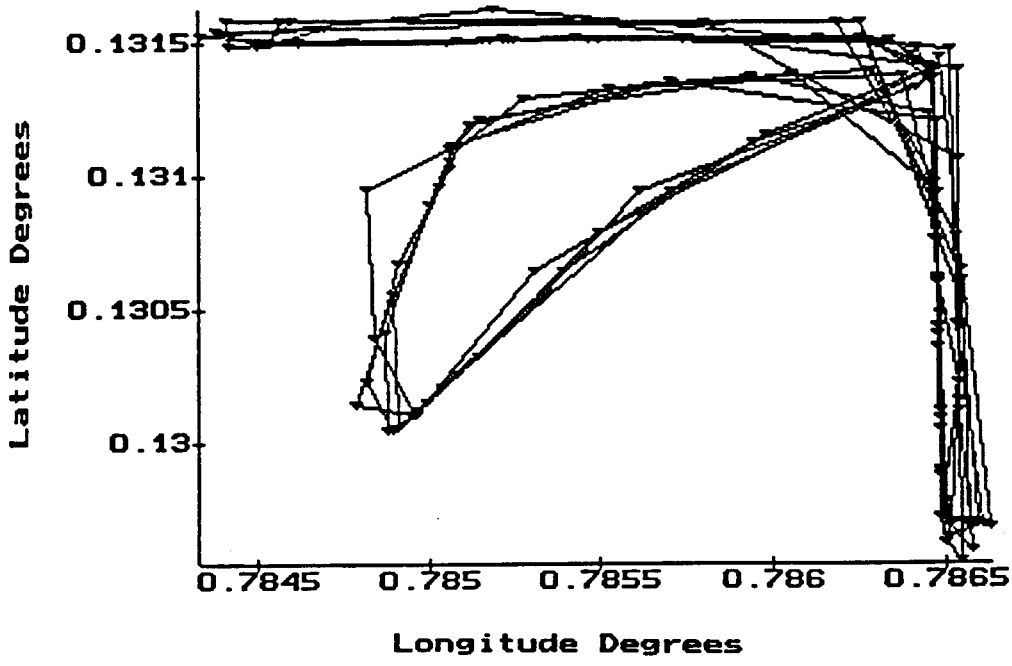

Figure 6.--Horizontal plot of kinematic trajectory for experiment B, February 17, 1991.

There are two traditional ways to initialize the processing of the entire trajectory (moving and/or static): (1) antenna swap and (2) known rover-start mark. These techniques are fully described in the references (refer back to the section on theory for the case where the rover-start mark is known). In short, there are proven static initialization methods for determining the integer ambiguities associated with a kinematic trajectory. Once these integers or lanes are established then the remainder of the trajectory can be generated with centimeter-level accuracy. This assumes no cycle slips.

If occasional cycle slips occur, they can be fixed as a part of the trajectory processing. If there are too many cycle slips the trajectory cannot be continued through that point and must be recovered backwards from a later time point. Although dealing with cycle slips is important, it is not an important aspect of this investigation. Here we use kinematic GPS with static initialization to precisely establish the truth trajectory.

Given that trajectory truth is therefore known, we subsequently reprocess the data using OTF methodology. This is also an initialization method but one that does not require a static step. As a matter of fact the OTF postprocessing software does not recognize the difference between static and kinematic points on the trajectory.

Thus, in the method used here, an arbitrary reference time is selected (with no consideration given to whether the rover was stopped or moving) with an associated period (forward and/or backwards) of the trajectory, to aid in obtaining a position estimate from carrier-smoothed

pseudoranges. For example, I would expect a 30-minute segment of the trajectory (largely free of cycle slips) to yield the trajectory position, at the selected reference time, to better than 2 m. Theoretically, this carrier-smoothed code processing step is not required. From a practical point of view, however, it is essential. The reason for this is simple. The initial guess of the trajectory position at t_{ref} establishes an origin around which to perform a search for the correct lanes. A good first guess allows the search volume to be small. With C/A code carrier-code smoothing, a typical search volume might be 64 m cubed (±2 m box) or possibly 216 m cubed (±3 m box). Without the carrier-code smoothing method, or some equivalent, the search volume might be a thousand times larger. Once the correct lanes have been uncovered, any neighboring portion of the trajectory, forward or backwards, up to problematic cycle slips, can be generated with centimeter accuracy.

In summary, I use kinematic GPS with static initialization to establish the truth trajectory. Then I use kinematic GPS without static initialization, described in this paper, to generate all or part of the trajectory. The two trajectories are then compared. As will be seen, in the remainder of this paper, the trajectories agree a the centimeter level.

.

In experiment A the OTF technique will generate the same trajectory as the traditional method. In experiment B, I generate the truth trajectory using nearby NBS3 as the static reference receiver. Thus, for OTF processing from NBS3 to the ROVER the same trajectory will be generated. On the other hand, when OTF processing is used to generate the SCHL-to-ROVER trajectory or the CLRK-to-ROVER trajectory one can expect few-centimeter level variations when they are compared with the truth trajectory.

For each of the two experiments I arbitrarily adopt a set of reference epochs and associated neighboring trajectory time segments. Table 5 lists seven cases to be processed for experiment A; table 6 lists 21 cases to be processed for experiment B. For experiment B the same 21 cases will apply for OTF processing of NBS3 to ROVER, SCHL to ROVER, and CLRK to ROVER.

Table 5.--Selected cases for OTF processing for experiment A, July 16, 1990

Case	Reference epoch	Early epoch	Late epoch	PDOP	Deltat (sec)	Span (min)	No. sats
1	3	----	100	3.02	15	24.25	5
2	3	----	50	3.02	15	11.75	5
3	176	----	232	3.40	15	14.00	6
4	176	----	200	3.40	15	6.00	6
5	176	----	192	3.40	15	4.00	6
6	306	260	----	5.05	15	11.50	6
7	306	298	----	5.05	15	2.00	6

I shall now explain the entries in tables 5 and 6. Consider case 3 from table 6. The selected reference epoch is 52 which, in this case, is 1040 seconds from the beginning of the data. "Early epoch" is 0. This indicates that epochs 0 - 52 will be mapped to epoch 52. "Late epoch" is 190.

This indicates that epochs 52 - 190 will be mapped back to epoch 52. Should one of these entries be dashed then the mapping is either forward or backward but not both. Here mapping has two connotations. First the code is carrier-mapped to the reference epoch. For codeless L2 C/A code receivers I have, so far, used only the L1 carrier for this mapping due to too many cycle slips on the squared L2 carrier. (It is true that these L2 cycle slips can often be fixed. This, however, was not an important part of this phase of the investigation and will be considered in the next phase.) Mapping also means that once the correct L1 ambiguities have been established, kinematic GPS is used to compute the trajectory over this same interval. Clearly I could have continued to compute the trajectory beyond this interval since the ambiguities still apply, but I have simply chosen not to do so.

Table 6.--Selected cases for OTF processing for experiment B, February 17, 1991

Case	Reference epoch	Early epoch	Late epoch	PDOP	Deltat (sec)	Span (min)	No. sats
1	10	----	100	3.41	20	30.00	5/6/5
2	52	0	290	2.67	20	96.67	6/5-6/5
3	52	0	190	2.67	20	63.33	6/5-6/5
4	52	0	100	2.68	20	33.33	6/5-6/5
5	52	0	60	2.68	20	20.00	6/5-6
6	52	30	60	2.68	20	10.00	6/5-6
7	100	----	200	3.00	20	33.33	5
8	300	200	----	3.64	20	33.33	5
9	300	----	400	3.64	20	33.33	5/6/5
10	496	400	----	3.64	20	32.00	6/5
11	600	496	----	2.26	20	34.67	5/6
12	600	----	700	2.26	20	33.33	5/6
13	637	470	715	2.73	20	33.33	5/6-5
14	660	----	780	2.73	20	40.00	6
15	680	----	780	2.60	20	33.33	6
16	700	----	780	2.81	20	26.67	6
17	700	----	800	2.81	20	33.33	6
18	718	----	840	2.78	20	58.00	6/5
19	718	----	888	2.73	20	56.67	6/5
20	750	----	870	2.42	20	40.00	6/5
21	800	----	888	2.42	20	29.33	5

The column labeled PDOP is actually the PDOP at the reference time based on the three double difference planes used to define the candidate lanes. As a point of reference, a PDOP of 1.00 would be required for the double difference planes to be perpendicular. The next column, "Deltat (sec)," represents the selected epoch spacing for the case. The column labeled "Span (min)" represents the total time span of the observations used in the case. The last column, "No. Sats," indicates the number of satellites used while processing the case. If both forward and backward mappings are employed, there will be a separating dash between two sets. For example, 6/5-6/5 is interpreted to mean that when projecting backwards (from epoch 52) one first has six satellites and then five and when projecting forward (from epoch 52) one first has six satellites and then five.

RESULTS

Experiment A

All seven selected cases used for experiment A were processed using the 163-centimeter lane candidates and 19-centimeter lane candidates. Table 7 comprises the experiment A postprocessing results.

Table 7.--OTF processing results for experiment A, ROME to ROVER (0.0 - 1.4 km), July 16, 1990

Case	Mode	Dx (cm)	Dy (cm)	Dz (cm)	Peak1 (%)	Std-dev1 (cycles)	Peak2 (%)	Std-dev2 (cycles)	Success? (yes/no)
01	163	55	108	90	98.6	0.010	98.1	0.014	yes
01	19	55	108	90	98.7	0.009	98.6	0.010	no(2)
02	163	67	121	96	98.5	0.010	98.2	0.012	yes
02	19	67	121	96	98.9	0.009	98.5	0.010	no(7)
03	163	35	8	8	97.7	0.012	91.6	0.042	yes
03	19	35	8	8	97.7	0.012	97.4	0.014	yes
04	163	47	61	65	97.5	0.011	94.7	0.027	yes
04	19	47	61	65	97.5	0.011	97.5	0.019	yes
05	163	88	74	80	97.2	0.011	94.1	0.024	yes
05	19	88	74	80	97.9	0.011	97.2	0.011	no(2)
06	163	26	21	117	97.1	0.015	90.4	0.026	yes
06	19	26	21	117	97.1	0.015	95.1	0.020	yes
07	163	36	150	204	98.6	0.009	92.9	0.021	yes
07	19	36	150	204	98.6	0.009	98.1	0.008	yes

Column 1 references the case number, referenced to table 5, and column 2 indicates whether 19-centimeter or 163-centimeter mode was used in generating the lane candidates. Columns 3, 4, and 5 (i.e., Dx, Dy, Dz) represent how closely the carrier-code-mapping method attained the established truth. The results are accurate to roughly 150 cm. The exception is case 7 where there is a time span of just 2.00 minutes. Typically 100-centimeter values can be expected as long as there is an ample number of epochs (e.g., 200), five or more satellites are available, a time span of 30 minutes is available for the carrier-code mapping, and the PDOP is normal.

The subsequent pair of columns, labeled "peak1" and "std-dev1" represent the ratio (given in percent) of the maximum peak with the maximum possible theoretical value and the standard deviation of the real-valued double difference ambiguities, computed at each epoch. The next pair of columns have similar information for the second highest peak when the previous two columns actually contain the correct peak. Otherwise these columns show the peak associated with the correct lanes. In this latter case one must refer to the column labeled "Success ?" to learn which peak holds the correct lanes. Stated differently, if the "Success ?" column is "yes," then "peak1" was in fact the peak with the correct lanes.

In this experiment double-wide lane (163 cm) processing always yielded the correct 19-centimeter lanes whereas narrow-lane processing was successful for four out of seven times. In

some cases (e.g., case 2) even the double-wide lane mode barely achieved success. In case 2, an 11.75-minute time span comprising only five satellites was minimally adequate and, in case 7, a 2-minute time span comprising six satellites was clearly adequate. Note how little margin there is in 19-centimeter mode results for cases 3, 4, and 7. Operational systems will demand that first and second peaks be clearly distinct.

Experiment B

Recall that the cases which apply to experiment B were presented in table 6.

The initial estimate (reported in the Dx, Dy, and Dz columns) were based on 20-second epochs (for both 163-centimeter processing and 19-centimeter processing) and entered on the 19-centimeter lines in tables 8-10, below. Although not used as the first guess in the OTF processing, 2-second carrier-code mapping results have been placed in table 8-10 on the 163-centimeter line for comparison purposes.

NBS3 to ROVER

Table 8 lists the results for NBS3-to-ROVER processing. The initial guess, based on differential carrier-code smoothing, is similar to what was achieved in experiment A. It can be seen that roughly 100-centimeter results have been achieved. For 163-centimeter mode processing the first peaks are usually substantially superior to second peaks. In those cases where first and second peaks are close (e.g., case 7) the standard deviation can be decisive -- especially for short baselines. I want to emphasize that success, here, is used in a clinical sense; it does not imply that the margins would be sufficient in an operational mode.

OTF processing based on 19-centimeter processing was often successful. Note, however, 19-centimeter mode failed in four of 21 cases. Clearly these were cases of inferior geometry. Nevertheless, the separations between the first and second peak are much better for double-wide lane mode than for narrow-lane mode. This is particularly true of the margins on the standard deviations.

Probably the most important aspect of the NBS3-to-ROVER processing is that 163-centimeter processing was always successful. This is very encouraging since just one of the cases needs to be successful in order to recover the entire 5-hour trajectory. This is so in this experiment since there were no important cycle slips in the data.

SCHL to ROVER

Table 9 provides the results for the SCHL-to-ROVER processing. All cases were attempted using the 163-centimeter mode and the 19-centimeter mode.

The resulting trajectories agree approximately with the truth trajectory. In most cases the agreement is better than 3 cm in all components. In the worst cases the differences are as large as 5 cm. The single exception to this is the portion of the trajectory related to the large PDOP spike around epoch 200. At the high point of this spike, nearly 10 cm differences were experienced in the vertical component. This paragraph applies to the CLRK-to-ROVER results, cited below, as well.

For case 1, whose reference epoch is 10, 163-centimeter mode processing failed. The failure appeares to be due to bad L2 observations at epoch 10. This is suspected (but not yet verified) because 19-centimeter mode was successful. Case 1A was added, expressly, to demonstrate that wide-lane processing would have no difficulty moments later. Note that this additional case uses a subset of the data used in case 1. The reference epoch for case 1A is 15, only 100 seconds later than the attempt at epoch 10.

Table 8.--OTF processing results for experiment B, NBS3 to ROVER (0.5 km), February 17, 1991

Case	Mode	Dx (cm)	Dy (cm)	Dz (cm)	Peak1 (%)	Std-dev1 (cycles)	Peak2 (%)	Std-dev2 (cycles)	Success? (yes/no)
01	163	21	69	10	97.4	0.022	90.0	0.072	yes
01	19	18	17	46	97.4	0.022	95.1	0.033	yes
02	163	31	42	17	96.1	0.030	91.3	0.055	yes
02	19	46	17	33	98.3	0.014	91.5	0.063	yes
03	163	27	43	23	95.4	0.031	90.0	0.045	yes
03	19	55	41	43	98.1	0.016	95.1	0.065	yes
04	163	29	91	2	97.6	0.020	92.6	0.096	yes
04	19	12	54	57	97.6	0.020	96.3	0.094	yes
05	163	27	125	10	97.5	0.023	93.9	0.054	yes
05	19	10	34	67	97.6	0.036	97.5	0.023	no(4)
06	163	38	129	4	97.5	0.028	95.7	0.063	yes
06	19	17	47	93	97.6	0.042	97.5	0.028	no(4)
07	163	15	18	58	98.4	0.009	97.6	0.030	yes
07	19	2	31	67	98.4	0.009	98.1	0.010	yes
08	163	30	14	11	98.5	0.009	94.2	0.029	yes
08	19	5	33	25	98.5	0.009	98.4	0.013	yes
9	163	4	89	72	97.3	0.012	94.1	0.049	yes
9	19	15	121	9	97.3	0.012	96.1	0.023	yes
10	163	91	150	159	97.1	0.014	94.4	0.055	yes
10	19	21	64	85	97.1	0.014	95.6	0.030	yes
11	163	21	47	77	97.0	0.010	96.3	0.023	yes
11	19	25	51	89	97.9	0.019	97.9	0.010	no(6)
12	163	6	33	77	96.9	0.015	89.5	0.089	yes
12	19	25	44	108	96.9	0.015	94.1	0.050	yes
13	163	14	56	105	96.5	0.014	82.5	0.104	yes
13	19	7	59	106	96.5	0.014	89.6	0.110	yes
14	163	6	35	152	96.8	0.012	80.2	0.061	yes
14	19	4	47	86	96.8	0.012	90.5	0.025	yes
15	163	8	72	163	96.8	0.012	80.2	0.110	yes
15	19	1	52	80	96.8	0.012	91.3	0.057	yes
16	163	4	76	154	96.9	0.012	85.0	0.091	yes
16	19	2	43	65	96.9	0.012	93.0	0.033	yes
17	163	2	80	158	96.6	0.016	84.3	0.115	yes
17	19	6	60	99	96.6	0.016	92.2	0.035	yes
18	163	13	90	161	96.9	0.016	87.6	0.078	yes
18	19	18	63	74	96.9	0.016	90.9	0.058	yes
19	163	12	91	158	97.0	0.016	83.1	0.135	yes
19	19	29	81	114	97.0	0.016	90.1	0.035	yes
20	163	9	100	148	96.9	0.018	88.9	0.093	yes
20	19	31	93	123	96.9	0.018	95.9	0.034	yes
21	163	15	157	133	97.3	0.016	96.2	0.031	yes
21	19	41	136	101	98.2	0.014	97.3	0.016	no(6)

Case 1A was successful. Thus the failure at epoch 10 would not be an impediment to real-time operations as it is not critical, within a few minutes, when the lanes are established. Once the

lanes are established at epoch 15 one could recover the trajectory backwards to epoch 10, and earlier, using the L1 carrier phase observations. Case 1 was the only failure. Case 1A proves that the failure was due to bad data and not insufficient geometry.

Case 4 was not an outright failure. The top two peaks were rather close but clearly separated from the third peak. The standard deviation of the second peak was a factor of two better than that of the first peak; this is often decisive. Thus the peak associated with the correct lanes, while not apparent, could have been selected. At the least the superior standard deviation for peak 2 provides a warning against peak 1.

Table 9.--OTF processing results for experiment B, SCHL to ROVER (8 km), February 17, 1991

Case	Mode	Dx (cm)	Dy (cm)	Dz (cm)	Peak1 (%)	Std-dev1 (cycles)	Peak2 (%)	Std-dev2 (cycles)	Success? (yes/no)
01	163	6	167	30	89.5	0.049	89.2	0.083	no
01A	163	6	167	30	94.5	0.034	91.2	0.054	yes
01	19	11	241	66	94.7	0.034	92.6	0.031	yes
02	163	4	162	29	96.1	0.030	91.3	0.055	yes
02	19	54	17	33	96.1	0.030	91.3	0.055	no(2)
03	163	55	9	29	95.4	0.031	90.0	0.045	yes
03	19	55	41	43	95.4	0.031	94.2	0.057	yes
04	163	53	0	23	94.9	0.075	94.0	0.034	yes(2)
04	19	49	36	2	95.5	0.043	94.0	0.034	no(4)
05	163	51	22	22	97.1	0.028	93.7	0.053	yes
05	19	14	127	14	97.9	0.030	97.1	0.028	no(4)
06	163	1	55	40	97.1	0.027	94.7	0.072	yes
06	19	58	100	8	97.9	0.033	97.1	0.027	no(4)
07	163	13	39	45	96.4	0.025	95.8	0.033	yes
07	19	18	45	96	96.9	0.023	96.4	0.025	no(4)
08	163	9	28	72	97.1	0.025	91.7	0.071	yes
08	19	46	1	30	97.4	0.021	97.1	0.025	no(2)
09	163	15	55	87	96.2	0.021	93.8	0.043	yes
09	19	56	71	1	96.1	0.021	95.7	0.026	yes
10	163	10	23	7	95.3	0.026	93.7	0.052	yes
10	19	57	85	89	95.3	0.026	94.1	0.049	yes
11	163	26	31	37	96.9	0.024	95.9	0.022	yes
11	19	46	69	57	97.3	0.028	96.9	0.024	no(2)
12	163	38	68	59	95.4	0.029	90.8	0.066	yes
12	19	11	21	101	95.4	0.029	92.5	0.031	yes
13	163	0	17	60	94.2	0.028	83.5	0.099	yes
13	19	32	48	77	94.2	0.028	89.5	0.073	yes
14	163	21	40	68	93.5	0.033	81.8	0.114	yes
14	19	31	51	47	93.5	0.033	88.7	0.050	yes
15	163	16	56	106	93.2	0.034	82.2	0.075	yes
15	19	35	54	43	93.2	0.034	90.3	0.042	yes
16	163	22	69	116	93.4	0.035	85.4	0.088	yes
16	19	33	61	42	93.4	0.035	90.3	0.049	yes
17	163	32	114	48	93.7	0.034	83.6	0.122	yes
17	19	28	77	63	93.7	0.034	88.1	0.043	yes
18	163	15	97	77	95.0	0.038	82.3	0.119	yes
18	19	39	86	64	95.0	0.038	92.7	0.047	yes
19	163	8	6	63	95.5	0.034	--80%	cutoff--	yes
19	19	20	74	26	95.5	0.034	88.4	0.107	yes
20	163	8	94	64	96.3	0.031	91.2	0.061	yes
20	19	34	111	70	96.3	0.031	95.5	0.027	yes
21	163	14	115	83	97.6	0.018	96.3	0.031	yes
21	19	24	75	29	97.6	0.016	97.6	0.018	no(2)

Again, note that the results of the initial carrier-code mapping step were within about 100 cm in all components. More importantly, note that 163-centimeter mode processing was normally decisive. When the peaks are close the variances can be helpful; however there are exceptions. While cases 7 and 11 were clinically successful there was insufficient margin. Note also that 19-centimeter mode processing fared poorly in many cases. In case 6, for example, 19-centimeter processing placed the correct set of lanes in fourth place.

Table 10.--OTF processing results for experiment B, CLRK to ROVER (13 km), February 17, 1991

Case	Mode	Dx (cm)	Dy (cm)	Dz (cm)	Peak1 (%)	Std-dev1 (cycles)	Peak2 (%)	Std-dev2 (cycles)	Success? (yes/no)
01	163	6	167	30	90.5	0.036	88.6	0.048	yes
01	19	48	113	28	93.9	0.030	90.5	0.036	no(10)
02	163	4	162	29	93.8	0.037	88.3	0.073	yes
02	19	14	104	36	93.8	0.037	90.0	0.078	yes
03	163	55	9	29	91.6	0.032	90.1	0.046	yes
03	19	8	104	26	93.3	0.046	91.6	0.032	no(2)
04	163	53	0	23	91.6	0.085	89.3	0.037	no(3)
04	19	11	141	45	94.7	0.082	89.3	0.037	no(11)
05	163	51	22	22	97.7	0.090	93.2	0.024	no(3)
05	19	39	79	19	97.7	0.090	93.2	0.024	no(22)
06	163	1	55	40	97.7	0.037	93.2	0.024	no(5)
06	19	133	62	31	97.7	0.037	93.2	0.024	no(33)
07	163	13	39	45	94.5	0.076	93.0	0.024	no(12)
07	19	29	92	37	98.4	0.012	93.0	0.024	no(52)
08	163	9	28	72	96.9	0.021	93.6	0.049	yes
08	19	40	17	68	97.8	0.019	96.9	0.021	no(3)
09	163	15	55	87	95.3	0.018	94.5	0.047	yes
09	19	25	243	127	96.4	0.032	95.3	0.018	no(3)
10	163	10	23	7	95.9	0.023	93.4	0.057	yes
10	19	29	80	23	95.8	0.024	95.1	0.039	yes
11	163	26	31	37	96.4	0.023	95.7	0.036	yes
11	19	21	1	22	96.6	0.034	96.4	0.023	no(3)
12	163	38	68	59	94.7	0.031	89.8	0.062	yes
12	19	8	62	118	94.7	0.031	92.7	0.042	yes
13	163	0	17	60	93.1	0.028	84.3	0.120	yes
13	19	18	33	70	93.1	0.028	88.6	0.082	yes
14	163	21	40	68	88.8	0.052	82.7	0.051	yes
14	19	23	23	102	89.4	0.071	88.8	0.052	no(2)
15	163	16	56	106	88.0	0.052	84.1	0.108	yes
15	19	31	28	78	88.7	0.076	88.0	0.052	no(2)
16	163	22	69	116	86.8	0.051	86.8	0.085	yes
16	19	37	10	50	92.5	0.034	86.8	0.051	no(6)
17	163	32	114	48	86.9	0.049	85.3	0.103	yes
17	19	26	5	16	93.1	0.035	86.9	0.049	no(3)
18	163	15	97	77	87.2	0.081	83.6	0.076	no
18A	163	18	3	33	88.3	0.060	87.4	0.081	yes
18	19	18	6	39	92.1	0.049	90.5	0.048	no
19	163	8	6	63	--80%	cutoff--	--80%	cutoff--	n/a
19A	163	17	52	35	90.0	0.061	81.6	0.156	yes
19	19	17	51	31	91.6	0.049	88.5	0.054	no
20	163	8	94	64	91.3	0.060	90.4	0.056	yes
20	19	4	36	18	93.9	0.043	91.3	0.060	no(6)
21	163	14	115	83	95.2	0.040	94.9	0.037	no(3)
21	19	7	148	79	96.5	0.030	95.2	0.040	no(11)

CLRK to ROVER

Table 10 gives results of the 13-kilometer CLRK to ROVER OTF postprocessing. These results are similar to the SCHL-to-ROVER results as stated earlier. As expected the peaks are somewhat diminished and the standard deviations are somewhat larger. Otherwise 163-centimeter mode processing was successful with a few exceptions.

Cases 4, 5, 6, and 7 were not successful for 163-centimeter mode. Interestingly, for these cases, peaks 3, 3, 5, and 12, respectively, were the correct peaks, and, in all of these cases, the standard deviations were the best. Clearly this implies that standard deviations provide additional information especially with regard to avoiding the wrong lanes.

The standard deviations associated with case 18 in 163-centimeter processing were abnormally poor and provided a similar warning. In fact this case was successfully rerun as case 18A just two epochs earlier (e.g., 40 seconds earlier) to verify there was sufficient geometry. In case 19 no peaks, at all, were found above our preset 80% threshold. This case, too, was rerun two epochs earlier and success was achieved. Because the correct solution did not appear, even as a lower peak, bad L1 phase measurements are suspected (this has not yet been verified). Obviously, the inability to establish correct lanes at occasional epochs would not adversely impact OTF operations. Cycle slips and insufficient geometry are the primary concerns.

Discussion

It should be noted that few statements of accuracy are included within this report because the emphasis is on establishing the lanes rather than accuracy. In all cases, however, successful lane resolution in experiment A implies the truth trajectory was achieved exactly or nearly exactly (i.e., within a couple of centimeters). In experiment B the same holds for the NBS3 to ROVER trajectory. For the longer trajectories there is typically 2 to 4 cm agreement. In the one brief period of poor PDOP, in experiment B, this approaches a decimeter. Also, correctness of lanes has been decided by the correctness of the trajectory at t_{ref}. This is equivalent to comparing lanes since the lanes were fixed to integers when the truth trajectory was established. In an operational environment the lanes will likely be monitored since, in the absence of cycle slips, they will remain constant in time.

It was not stated above, but initializing on the fly can be difficult at a PDOP spike (e.g., epoch 200 of figure 5). Positions derived from code pseudoranges are poor at the spike. Because carrier phase measurements are more precise than code pseudoranges, the kinematic GPS positional error will not be as large especially if the integer ambiguities are known. Nevertheless, attempts to perform OTF initialization at the spike will cause candidate solutions to be offset and the peaks will be correspondingly reduced making the correct lanes difficult to find. However, the standard deviations of the real-valued ambiguities might still be quite small. Although not included in the above tables, OTF initialization was unsuccessfully attempted at reference epoch 200. This case was not included in the tables because I believe evaluation of OTF methodology should not be based on success or failure at PDOP spikes. In a real-time or postprocessing situation PDOP spikes can be anticipated and avoided during the initialization step by selecting a different reference time. Note (refer to table 6) that the OTF initialization cases 7 (reference epoch 100) and 8 (reference epoch 300) in experiment B were successful.

Although accuracy was considered to be secondary in these results, I shall include a typical example. I shall compare the CLRK-to-ROVER case 12 OTF results with trajectory truth as described earlier. In case 12 the carrier-smoothed code first guess was good to 29 cm, 65 cm, and 89 cm in the x, y, and z components, respectively. This is a typical result. The correct peak was found without question. The L1 integer lanes were then used to generate the trajectory from epoch 600 to epoch 700. This trajectory was differenced with the truth trajectory. The component differences are plotted in figure 7 as easting, northing, and vertical differences in centimeters.

I have also performed OTF processing of experiment B using data at 2-second epochs but have not included the results in this report. As expected, there was no significant improvement in the ability to establish the lanes. I attribute this to the fact that, when 20-second epochs were used, there were an ample number of observation epochs.

Tropospheric modeling was applied in this investigation. On the other hand ionospheric modeling or the removal of ionospheric delays through the formation of the ionospherically-free data combination was not employed.

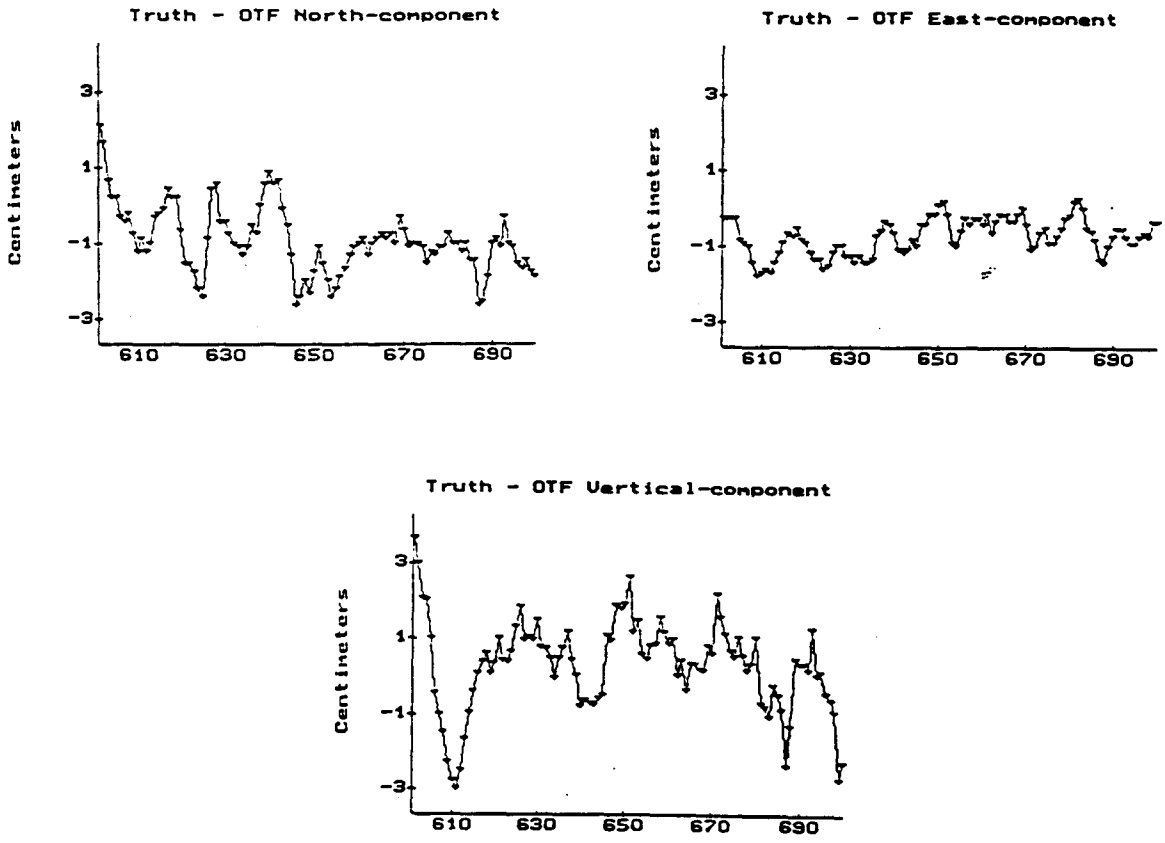

Figure 7.--OTF-generated kinematic trajectory from CLRK-to-ROVER processing minus trajectory truth from NBS3-to-ROVER processing, February 17, 1991.

FUTURE PLANS

I shall continue to process the experiments discussed here in assorted ways, including 19-centimeter, 34-centimeter, 43-centimeter, and 163-centimeter modes. These data will be processed at consecutive epochs using variable time spans. They will also be processed on an assortment of epoch intervals. These kinds of processing variations have already begun to be examined. Also the removal of ionospheric path delay will be included in the next phase of this investigation.

It is planned that all of the dozen or so experiments to date will be similarly processed and documented. In addition, the USACOE will be performing quasi-operational demonstrations of this technology in the months ahead. These experiments will be postprocessed along the lines of this report. Because so much processing is anticipated, the algorithms will be optimized. My goal is to perform the lane search within 1 second.

In addition to the above plans, I am working with USACOE and will be performing similar experiments over longer baselines (e.g., 25 km, 40 km, and perhaps longer). As the baseline lengths get longer we shall be giving increased consideration to modeling systematic effects with the aid of multiple reference stations.

SUMMARY

Many experiments have now been performed to investigate the limits of OTF kinematic GPS. This technique enhances the already powerful kinematic GPS with static initialization by processing methodology that allows the initialization to be accomplished while moving.

In this report two experiments were selected for processing using OTF methodology. These observations were first processed using proven methods in order to establish trajectory truth. Subsequently they were processed using new OTF postprocessing software and the results were compared.

Accuracy was not the primary result sought. More important than accuracy was the development of guidelines to establish what amount of data is required for success. Probably the most important factor is the number of satellites required. Next is the time span of data required to achieve the lanes with certainty. Highly important to many potential applications is the distance over which OTF processing is reliable.

There are many secondary issues as well: (1) Does high-rate sampling aid in the process of establishing the lanes? (2) What amount and variability of tropospheric and ionospheric delays can be tolerated? (3) How much advantage does P code receivers have over C/A receivers -- especially at the lower elevations.

In this report I have attempted to provide initial answers to the most important of these questions and, to a lesser extent, some of the secondary ones.

CONCLUSIONS

The following conclusions must be considered preliminary due to the limited amount of experience accumulated thus far.

The kinematic OTF GPS method works with just five satellites, but, with six satellites, the process is significantly stronger.

Success over the 0.5 to 1.4 km baselines was resounding. Even short-distance OTF can be useful for certain applications. Simplifying the before-takeoff and after-landing aspects of photogrammetric surveys provides one example. Eliminating the antenna-swap step in certain water-going or land surveys suggests others.

These results were derived from data collected under benign conditions. Nevertheless, they suggest that OTF operations out to 13 km should be readily achievable. I believe they also suggest that OTF will perform adequately out to at least 20 km to 30 km under favorable conditions. With hours of data, free of cycle slips, even longer baselines should pose no problem for dual frequency C/A code receivers.

The additional L2 signal strength achieved by P code receivers will give them an important advantage with respect to OTF technology. This is because P code receivers have a lower L2 operating elevation than do C/A code receivers. In a constellation of 24 GPS satellites, there are typically seven or eight satellites above 5° elevation.

I have demonstrated that the double-wide lane works and is better able to discriminate the lanes than narrow-lane processing. In fact, the Doppler signal over 163 cm will be 8.5 times as strong as that over 19 cm and 4.8 times as strong as that over 34 cm.

I have suggested that while it may not be possible to establish the L1 lanes at every epoch using double-wide lane processing, this should not pose a problem for real-time operations. However, assuming an adequate data set, an OTF method should be expected to find the lanes at most reference epochs.

I have found that there is only a modest improvement to the carrier-smoothed-code-generated first guess with sample rates greater than once per 20 seconds. I have also shown that a high sample rate provides little aid in establishing the lanes. This is to be expected. More important, to both of these processes, are an adequate number of epochs and an adequate time span.

ACKNOWLEDGEMENTS

I would like to recognize Mr. Stephen R. DeLoach for his foresight and leadership as a key promoter and as a provider of the means to this technology. Many individuals have supported this investigation in widely different capacities: from the USACOE Mr. Carl Lanigan, Mr. Fred Gloeckler, Mr. Bryn Fosburgh, and Mr. Jeff Walker; from NOAA Rear Admiral J. Austin Yeager, Captain Melvyn C. Grunthal, Captain A. Nicholas Bodnar (retired), Mr. Harold G.

Beard, personnel from field party G-3, and many others; from NIST, Mr. Charles J. Fronczek. Finally I would like to acknowledge that this project is supported by funds from the Dredging Research Program of the USACOE.

REFERENCES

Deloach, S.R., 1991: Precise real-time dredge positioning. GPS World, Vol. 2, No. 2, pp. 43-45, February.

Hatch, R.R., 1982: The synergism of GPS code and carrier measurements. Magnavox Advanced Products and Systems Company, Torrence, CA.

Hatch, R.R., 1990: Instantaneous ambiguity resolution. KIS Symposium 1990, Banff, Canada, September.

Hein, G.W., Landau, H., and Blomenhofer, H., 1990: Determination of instantaneous sea surface, wave heights, and ocean currents using satellite observations of the Global Positioning System. Institute of Astronomical and Physical Geodesy (IAPG), University FAF Munich, Neubiberg, Germany.

Hwang, P.Y.C., 1990: Kinematic GPS: resolving integer ambiguities on the fly. IEEE Position Location and Navigation Symposium, Las Vegas, NV, March 20-23, pp. 579-586.

Loomis, P., 1989: A kinematic GPS double differencing algorithm. Proceedings of the Fifth International Symposium on Satellite Positioning, Las Cruces, NM, pp. 611-620.

Mader, G.L., 1990: Ambiguity function techniques for GPS phase initialization and kinematic solutions. Proceedings of the Second International Symposium on Precise Positioning with the Global Positioning System, Ottawa, Canada, September 3-7, pp. 1233-1247.

Remondi, B.W., 1990: Pseudo-kinematic GPS using the ambiguity function method. NOAA Technical Memorandum NOS NGS-52, National Geodetic Information Center, Rockville, MD, May, 1990.

Remondi, B.W., 1985a: Global Positioning System carrier phase: description and use. Bulletin Géodésique, 59, pp. 361-377, January.

Remondi, B.W., 1985b: Performing centimeter-level surveys in seconds with GPS carrier phase: Initial results, Navigation, Vol. 32, No. 4, Winter 1985-1986.

Remondi, B.W., 1988: Kinematic and pseudo-kinematic GPS. Proceedings of the Satellite Division's International Technical meeting, The Institute of Navigation, Colorado Springs, CO, September 19-23, 115-121.

Rocken, C., Kelecy, T., Born, G., Young, L., Purcell, G., and Wolf, K. 1990: Measuring precise sea level from a buoy using the Global Positioning System. Geophysical Research Letters, Vol. 17, No. 12, 2145-2148, November.

Seeber, G. and Wubbena, G., 1989: Kinematic positioning with carrier phase and "On the way" ambiguity solution. Proceedings of the Fifth International Geodetic Symposium on Satellite Positioning, Vol. II, Las Cruces, NM, March 13-17.

PRODUCT DISCLAIMER

Mention of a commercial company or product does not constitute an endorsement by the National Oceanic and Atmospheric Administration. Use for publicity or advertisement purposes of information from this publication concerning proprietary products or the tests of such products is not authorized.